HHS Public Access

Author manuscript

ACS Biomater Sci Eng. Author manuscript; available in PMC 2024 August 14.

Published in final edited form as:

ACS Biomater Sci Eng. 2023 August 14; 9(8): 4916–4928. doi:10.1021/acsbiomaterials.3c00290.

Inflammatory Licensed hMSCs Exhibit Enhanced Immunomodulatory Capacity in a Biomaterial Mediated Manner

Vasiliki Kolliopoulos,
Department of Chemical and Biomolecular Engineering, University of Illinois at Urbana–Champaign, Urbana, Illinois 61801, United States

Maxwell Polanek,
Department of Chemical and Biomolecular Engineering, University of Illinois at Urbana–Champaign, Urbana, Illinois 61801, United States

Hui Xu,
Tumor Engineering and Phenotyping (TEP) Shared Resource, Cancer Center at Illinois, University of Illinois Urbana–Champaign, Urbana, Illinois 61801, United States

Brendan Harley
Department of Chemical and Biomolecular Engineering, University of Illinois at Urbana–Champaign, Urbana, Illinois 61801, United States; Cancer Center at Illinois, University of Illinois at Urbana–Champaign, Urbana, Illinois 61801, United States; Carl R. Woese Institute for Genomic Biology, University of Illinois at Urbana–Champaign, Urbana, Illinois 61801, United States

Abstract

Craniomaxillofacial (CMF) bone injuries represent particularly challenging environments for regenerative healing due to their large sizes, irregular and unique defect shapes, angiogenic requirements, and mechanical stabilization needs. These defects also exhibit a heightened inflammatory environment that can complicate the healing process. This study investigates the influence of the initial inflammatory stance of human mesenchymal stem cells (hMSCs) on key osteogenic, angiogenic, and immunomodulatory criteria when cultured in a class of mineralized collagen scaffolds under development for CMF bone repair. We previously showed that changes in scaffold pore anisotropy and glycosaminoglycan content can significantly alter the regenerative activity of both MSCs and macrophages. While MSCs are known to adopt an immunomodulatory phenotype in response to inflammatory stimuli, here, we define the nature and persistence of MSC osteogenic, angiogenic, and immunomodulatory phenotypes in a 3D mineralized collagen

Corresponding Author: Brendan Harley – Department of Chemical and Biomolecular Engineering, University of Illinois at Urbana–Champaign, Urbana, Illinois 61801, United States; Cancer Center at Illinois, University of Illinois at Urbana–Champaign, Urbana, Illinois 61801, United States; Carl R. Woese Institute for Genomic Biology, University of Illinois at Urbana–Champaign, Urbana, Illinois 61801, United States; Phone: (217) 244-7112; bharley@illinois.edu; Fax: (217) 333-5052.

Author Contributions

Contributions (CRediT: Contributor Roles Taxonomy[51,52]): Vasiliki Kolliopoulos, Conceptualization, Data curation, Formal analysis, Visualization, Investigation, Methodology, Writing – original draft, Writing – review and editing; Maxwell Polanek, Investigation, Data curation, Formal analysis, Writing; Hui Xu, Investigation; Brendan Harley, Conceptualization, Resources, Project administration, Funding acquisition, Supervision, Writing – review and editing.

Complete contact information is available at: https://pubs.acs.org/10.1021/acsbiomaterials.3c00290

The authors declare no competing financial interest.

environment, and further, whether changes to scaffold architecture and organic composition can blunt or accentuate this response as a function of inflammatory licensing. Notably, we found that a one-time licensing treatment of MSCs induced higher immunomodulatory potential compared to basal MSCs as observed by sustained immunomodulatory gene expression throughout the first 7 days as well as an increase in immunomodulatory cytokine (PGE_2 and IL-6) expression throughout a 21-day culture period. Further, heparin scaffolds facilitated higher osteogenic cytokine secretion but lower immunomodulatory cytokine secretion compared to chondroitin-6-sulfate scaffolds. Anisotropic scaffolds facilitated higher secretion of both osteogenic protein OPG and immunomodulatory cytokines (PGE_2 and IL-6) compared to isotropic scaffolds. These results highlight the importance of scaffold properties on the sustained kinetics of cell response to an inflammatory stimulus. The development of a biomaterial scaffold capable of interfacing with hMSCs to facilitate both immunomodulatory and osteogenic responses is an essential next step to determining the quality and kinetics of craniofacial bone repair.

Graphical Abstract

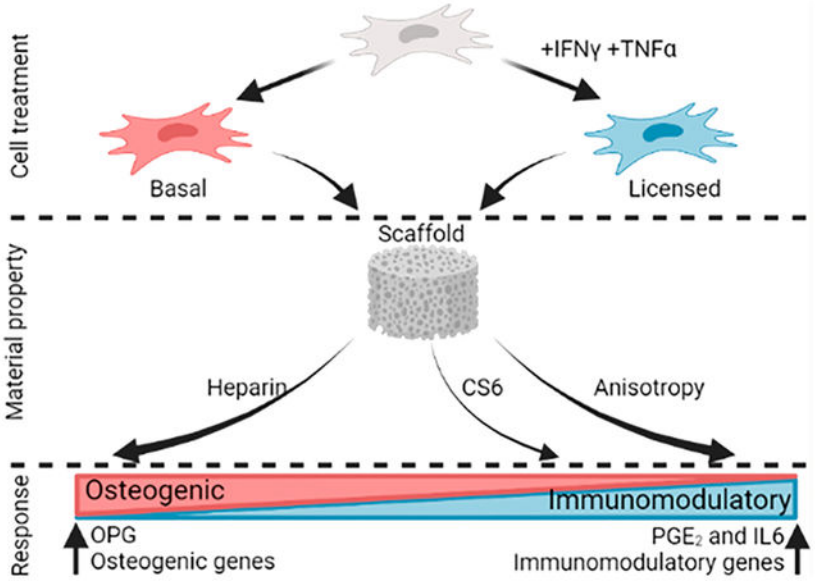

Keywords

mesenchymal stem cell; immunomodulation; osteogenesis; craniomaxillofacial defect; biomaterial

1. INTRODUCTION

Craniomaxillofacial bone defects pose an exceptionally difficult challenge for repair, as they are often irregular in size and shape. Current standards of repair include autografts, allografts and other biomaterial implants.[1] However, the success of these grafts varies due to age-related regenerative potential among other factors.[2–4] An alternative reparative strategy would be to deliver an osteoinductive biomaterial implant that could promote regenerative healing *via* processes linked to osteoprogenitor recruitment, differentiation, and matrix

remodeling, *via* vascular repair, and *via* modulation of the complex immune environment after injury.

Mesenchymal stem cells (MSCs) are an attractive cell source for CMF bone repair applications, as they have potential to expand and differentiate into osteogenic lineages. MSCs may also contribute to tissue regeneration as powerful factories of biomolecules that can promote other processes essential for regenerative healing such as angiogenesis, vascular remodeling, and, increasingly, immunoregulation. However, it is increasingly believed MSCs do not elicit strong immunomodulatory activity until they are first activated or "licensed" by inflammatory cytokines such as interferon-γ (IFN-γ) and tumor necrosis factor alpha (TNF-α) secreted by immune cells like macrophages at the wound site.[5–8] MSCs subsequently exert immunomodulatory effects both indirectly via the production of soluble mediators such as prostaglandin E_2 (PGE_2) and interleukin-6 (IL-6) as well as via direct cell-cell contact.[5,8–10] PGE_2 is produced by MSCs under inflammatory conditions and influences the activation, proliferation, differentiation and function of immune cells from both adaptive and innate immunity.[10] IL-6 has recently been described as having a "two-sided" engagement in immunomodulation possessing both pro- and anti-inflammatory properties.[11,12] IL-6 is established to be the basic cytokine responsible for MSC immunoregulatory effects; however, MSCs can be both a source and a target of these effects.[10] Numerous studies have focused on the effects of these soluble immunomodulatory mediators on MSCs; however, the influences of bone mimetic extracellular matrix on the interplay of MSC immunomodulatory and osteogenic potential remains understudied.

We are developing a mineralized collagen biomaterial to promote MSC recruitment, osteogenic differentiation, and immunomodulatory activity for CMF bone regeneration applications. A critical characteristic of this scaffold is its ability to induce mineral and bone formation *in vivo* without the use of exogenously added osteogenic supplements.[13–22] While originally developed with *in vivo* applications in mind, the well-characterized scaffold environment increasingly provides a platform to interrogate the role of scaffold architecture, composition, and mechanics on multicellular signaling processes that occur in the context of regenerative healing and homeostasis. We have developed methods to fabricate these scaffolds with various anisotropies and pore sizes that increase cell metabolic activity, provide directional growth in nonmineralized scaffold variants, and provide increased cell migration and bone formation in mineralized variants.[23–28] Recently we showed mineralized collagen scaffolds containing glycosaminoglycans such as chondroitin-6-sulfate (CS6), chondroitin-4-sulfate, and heparin sulfate (Hep) on MSC-induced osteogenic differentiation, mineral formation, angiogenesis and monocyte differentiation.[23,29] We observed that heparin scaffolds elicited the greatest potential for osteoclast inhibition via the production of osteoprotegerin (OPG), a decoy receptor binding to RANK ligand (RANKL) preventing the development of functionally active osteo-clasts,[29,30] while CS6 scaffolds displayed greatest potential in enhancing angiogenesis. Interestingly, all mineralized collagen scaffold variants hinted to an immunosuppressive effect leading to limited pro- and anti-inflammatory macrophage protein secretion.[29] Furthermore, CS6 scaffolds promoted the greatest M1 to M2 gene expression transition indicating a potential to mitigate the pro-inflammatory immune environment.[29] However, there is limited understanding of how

glycosaminoglycans influence MSC immunomodulatory potential and how these can be harnessed to direct immune cell fate in the surrounding microenvironment.

Here we examine the influence of MSC licensing on the potential for mineralized collagen scaffolds to bias MSC osteogenic differentiation and immunomodulatory potential. Based on prior observations using nonlicensed MSCs, we expected that while Heparin containing scaffolds may enhance osteogenic response, anisotropic scaffolds will promote an immunomodulatory phenotype. Using in vitro culture approaches, we compare osteogenic and immunomodulatory potential of MSCs maintained in basal conditions versus those briefly licensed before subsequently maintained in basal conditions in mineralized collagen scaffolds as a function of scaffold glycosaminoglycan composition and pore anisotropy over a 21-day culture period. The studies provide important insight regarding the ability for scaffold structural and composition features to improve osteogenic and immunomodulatory responses for MSCs within an inflammatory wound environment. These studies also provide an important description of the multiweek time scale over which the effects of a single inflammatory stimuli to MSCs can persist in the form of extended alterations to MSC osteogenic and immunomodulatory phenotype.

2. MATERIALS AND METHODS

2.1. Experimental Design.

This study aimed to identify the effect of mineralized collagen scaffold composition and pore structure on MSC osteogenesis and immunomodulation in the presence or absence of initial inflammatory stimuli and elucidate a possible approach for biomaterial design to mediate MSC trophic signals (Figure 1). Human mesenchymal stem cells were licensed with a single stimulus one day prior to seeding on mineralized collagen scaffolds. Mineralized collagen scaffolds with isotropic pores containing chondroitin-6-sulfate (CS6 Iso) were compared against a glycosaminoglycan variant (Hep Iso) and an anisotropic variant (CS6 Ani). These scaffolds were cultured with basal or licensed human mesenchymal stem cells for 21 days in basal conditions. We assessed the role of scaffold design compared to MSC licensing on key markers of hMSC regenerative phenotype for 21 days of culture: hMSC metabolic activity *via* the AlamarBlue assay; secretion of hMSC osteogenic and immunomodulatory factors *via* ELISAs; expression of key osteogenic and immunomodulatory genes *via* NanoString.

2.2. Fabrication of Mineralized Collagen-Glycosaminoglycan Scaffolds with Varying Glycosaminoglycan Content and Pore Structure.

Mineralized collagen-glycosaminoglycan scaffolds were fabricated from a mineralized collagen precursor suspension with one of two glycosaminoglycans, chondroitin-6-sulfate (CS6) or heparin (Hep), as previously described.[14,23,29,31] Type I bovine collagen (1.9 w/v% Collagen Matrix Inc., New Jersey USA), calcium salts (calcium hydroxide and calcium nitrate tetrahydrate, Sigma-Aldrich), and glycosaminoglycans (0.84 w/v%, CS6: Chondroitin sulfate sodium salt, CAS 9082–07–9, Spectrum Chemicals, or Hep: Heparin sodium salt from porcine intestinal mucosa, CAS 9041–08–1, Sigma-Aldrich) was homogenized in mineral buffer solution (0.1456 M phosphoric acid/0.037 M calcium

hydroxide). The mineralized collagen precursor suspension was then transferred to aluminum molds and lyophilized into porous isotropic scaffolds using a Genesis freeze-dryer (VirTis, Gardener, New York USA). During the lyophilization process, the suspensions were cooled at a constant rate of 1 °C/min from 20 to −10 °C followed by a hold at −10 °C for 2 h. Following freezing, the ice crystals within the suspension were then sublimated at 0 °C and 0.2 Torr, resulting in a porous scaffold network. A 6 mm diameter biopsy punch (Integra LifeSciences, New Jersey, USA) was used to create the individual scaffolds.

To generate mineralized collagen scaffolds with anisotropic pores, the mineralized collagen precursor suspension containing CS6 glycosaminoglycan was transferred to a Teflon mold with a copper base. These followed the same lyophilization protocol as that described above. The difference in heat transfer coefficients of Teflon and copper results in unidirectional heat transfer and in an anisotropic pore network. Previous work has thoroughly characterized these mineralized collagen scaffold variants as seen in Figure 1.[23,24,32–34] We have previously shown that all scaffold variants described herein have an approximately 180 μm pore diameter. By varying glycosaminoglycan, there is no difference in pore anisotropy or stiffness.[32,33] However, by varying pore anisotropy materials display elongated pores and increased bulk stiffness.[23]

2.3. Sterilization, Hydration, and Scaffold Cross-linking.

All scaffolds were sterilized via ethylene oxide treatment for 12 h using an AN74i Anprolene gas sterilizer (Andersen Sterilizers Inc., Haw River, North Carolina USA) after being placed in sterilization pouches. Following sterilization, all subsequent steps were conducted in an aseptic environments. Sterile scaffolds were hydrated and cross-linked using EDC-NHS chemistry as previously described.[23,24,29,35] Scaffolds were first soaked in 100% sterile ethanol, followed by washes and a soak in phosphate-buffered saline (PBS). The scaffolds were then cross-linked by EDC-NHS followed by further PBS washed and finally soaked in basal growth media for 48 h prior to cell seeding.

2.4. Cell Culture, Priming, and Seeding of Human Mesenchymal Stem Cells on Mineralized Collagen Scaffolds.

2.4.1. Human Mesenchymal Stem Cell Culture and Priming.—Passage 4 marrow human mesenchymal stem cells (hMSCs) of a 20 year old African American female (RoosterBio, Frederick, MD, USA) were expanded to passage 5 using RoosterNurish expansion media for the first 3 days followed by 3 more days of culture media containing low glucose DMEM and glutamine, 10% mesenchymal stem cell fetal bovine serum (Gemini, California, USA), and 1% antibiotic-antimycotic (Gibco, Massachusetts, USA) in an incubator at 37 °C and 5% CO_2. hMSCs were licensed with inflammatory stimuli 20 ng/mL IFN-γ and 10 ng/mL TNF-α (cyt-206 and cyt-223 respectively, ProSpec Protein Specialists) on day 5 of culture for 24 h prior to seeding onto the scaffolds.

2.4.2. Human Mesenchymal Stem Cell Seeding on Mineralized Collagen Scaffolds.—Hydrated mineralized collagen scaffolds containing either chondroitin-6-sulfate (CS6) with isotropic or anisotropic pores (Iso or Ani) or heparin (Hep) with isotropic pores were seeded at a density of 150,000 cells per scaffold with either basal or licensed

cells. Briefly, basal and licensed cells were lifted from T175 flasks using TrypLE Express Enzyme (Thermo Fisher Scientific, Waltham, MA, USA) for 5 min in an incubator at 37 °C and 5% CO_2 followed by tapping. An equal amount of culture media was used to neutralize the TrypLE. Cells were pelleted by spinning at 200 g for 10 min and resuspended with culture media to a final concentration of 150,000 cells/mL. Six hydrated scaffolds of each type were placed in a six-well plate with 6 mL of basal or licensed cells. These were then placed on a shaker in an incubator at 37 °C and 5% CO_2 for 6 h. Cell seeded scaffolds were then removed from the 6-well plate and placed in 24-well plates supplemented with 1 mL/well of culture media for the rest of the experiment. Cells remaining in the 6-well plate were counted using a Countess Automated Cell Counter (Invitrogen, Waltham, MA, USA) to confirm seeding of the scaffolds.

2.5. Cell Metabolic Activity Quantification.

Cell viability was quantified through a nondestructive metabolic activity alamarBlue assay (Invitrogen, Carlsbad, CA, USA) at days 3, 7, 14, and 21 of culture ($n = 4$) (Figures 2A and 4A). Scaffolds were soaked in alamarBlue as per manufacturer's instructions in an incubator for 1.5 h under gentle shaking. Following the incubation, the alamarBlue solution was fluorescently measured using a F200 spectrophotometer (Tecan, Mannedorf, Switzerland) for the presence of resorufin (540 (52-nm excitation), 580 (20-nm emission)). Metabolic activity was calculated from a standard curve generated from a known number of cells at day 0, normalized to the initial seeding density of 150,000 cells per scaffold.

2.6. Quantification of Osteogenic and Immunomodulatory Factors Secreted.

Osteoprotegerin (OPG) an osteogenic factor secreted by hMSCs, known to inhibit osteoclastogenesis and immunomodulatory factors such as IL-6 and PGE_2 were quantified via their respective ELISAs (OPG – DY805, IL-6 – DY206, PGE_2 – KGE004B, R&D Systems, Minneapolis, MN, USA) (Figures 2B–D and 4B–D). Media were collected every 3 days throughout the 21-day culture period and then pooled (day 3; day 6 and 9; day 12 and 15; day 18 and 21) to generate a cumulative release profile for analysis, comparing the result to a blank media control ($n = 5$).

2.7. RNA Isolation and NanoString Gene Expression Analysis from Cell-Seeded Scaffolds.

Cell-seeded scaffolds were harvested for RNA isolation on days 3, 7, 14, and 21 ($n = 3$). Each cell-seeded scaffold was cut in quarters and placed into a phasemaker tube (ThermoFisher Scientific, Massachusetts, USA). To each tube 1 mL of TRIzol Reagent (ThermoFisher Scientific, Massachusetts, USA) was added and vortexed briefly. Next, 200 μL of chloroform was added to each tube, vortexed, and allowed to sit for 5 min at room temperature. The tubes were then centrifuged at 15,000 g for 15 min at 4 °C. The supernatant was then diluted in 1:2 with 100% ethanol prior to continuing with a conventional isolation protocol using the RNEasy mini kit (Qiagen) per manufacturer's instructions. RNA concentration was measured using a NanoDrop spectrophotometer.

A custom NanoString panel of 38 mRNA probes was used to quantify the transcript expression with the NanoString nCounter System (NanoString Technologies, Inc.) with

the NanoString nCounter System (NanoString Technologies, Inc.) located at the Tumor Engineering and Phenotyping Shared Resource (TEP) at the Cancer Center at Illinois (Supp. Table 1). The nSolver Analysis Software (NanoString Technologies, Inc.) was used for data processing, normalization, and evaluation of expression. Raw data was normalized to a day 0 basal control ($n = 3$) and expression levels are depicted as a fold change (Figures 3 and 5). Day 0 values of RNA expression for licensed MSCs were also expressed as a fold change to day 0 basal (Supp. Table 2).

2.8. Statistics.

Statistics were performed using OriginPro (OriginPro, Massachusetts, USA and RStudio (RStudio, Massachusetts, USA) software. Significance was set to $p < 0.05$. First, a Shapiro-Wilk test was used to test for normality, followed by a Grubbs test to remove outliers if data was not normal. If removal of outliers did not result in normal data, the outlier was not removed from the data set. A Levene's test was also performed to test the equal variance assumption. For normal data with equal variance, a two-way ANOVA was used to assess significance. If data for a given time point was not normal, had unequal variance, or both, statistics were done separately on each hMSC treatment (basal or inflammatory). First, a Shapiro-Wilk test was used to test for normality. Then a Levene's test was performed to test the equal variance assumption. If data was normal and had equal variance, a one-way ANOVA with a Tukey posthoc test was performed. If data was normal but had unequal variance, a one-way Welch's ANOVA and Welch/Games-Howell posthoc was performed to determine significance. In the case of non-normal data with unequal variance, a Welch's Heteroscedastic F test and Welch/Games-Howell posthoc were performed. Finally, if data was non-normal but had equal variance, a Kruskal–Wallis test was used. Error bars for all data are represented as mean ± standard deviation, and all graphs were made in OriginPro.

3. RESULTS

3.1. Inclusion of Heparin As the Glycosaminoglycan in Mineralized Collagen Scaffolds Does Not Enhance hMSC Metabolic Activity.

Licensing drives metabolic activity with a significantly ($p < 0.05$) greater response observed on day 21 for both scaffold compositions (Figure 2A). Furthermore, we observed no significant differences in metabolic activity between chondroitin-6-sulfate containing scaffolds and heparin scaffolds within the same cell treatment throughout the 21-day period, indicating glycosaminoglycan type is not a driving factor in MSC metabolic activity.

3.2. Osteoprotegerin Secretion by hMSCs Is Significantly Enhanced with the Inclusion of Heparin.

Licensing displayed a strong influence on the production of OPG in early stages of culture in a glycosaminoglycan dependent manner (Figure 2B). Specifically, heparin scaffolds containing licensed MSCs expressed significantly higher ($p < 0.05$) amounts of OPG compared to all other scaffolds and cell treatments on days 3 and 9. However, glycosaminoglycan type was the driving force for OPG production. Throughout the 21-day culture period, heparin containing scaffolds regardless of cell treatment expressed significantly higher ($p < 0.05$) amounts of OPG compared to the chondroitin-6-sulfate

scaffolds, with an exception on the day 9 basal condition. On days 15 through 21 heparin scaffolds containing basal cells expressed significantly higher ($p < 0.05$) amounts of OPG compared to all other scaffolds and cell treatments.

3.3. Licensed Cells Seeded on Chondroitin-6-sulfate Mineralized Collagen Scaffolds Express Higher Amounts of Immunomodulatory Cytokines Compared to Heparin Scaffolds.

We observed an increased expression of both soluble PGE_2 and IL-6 in the licensed scaffold groups throughout the 21 day culture (Figure 2C–D). Specifically, chondroitin-6-suflate scaffolds with licensed MSCs expressed significantly more PGE_2 ($p < 0.05$) compared to basal conditions on days 15 through 21. However, there was no significance in PGE_2 expression between chondroitin-6-sulfate and heparin scaffolds in the same cell treatment. Licensed MSCs in heparin scaffolds significantly decreased IL-6 production ($p < 0.05$) compared to chondroitin-6-sulfate scaffolds throughout the 21-day culture period. Furthermore, chondroitin-6-sulfate scaffolds seeded with licensed cells expressed significantly ($p < 0.05$) more IL-6 than both basal scaffold groups on day 15.

3.4. NanoString Osteogenic Gene Expression Reveals hMSC Treatment Supersedes Scaffold Composition.

Licensing hMSCs increases the overall osteogenic gene expression profile compared to the basal cells, as seen in 10 out of the 19 osteogenic genes at day 0, Figure 3A,B. Seeding hMSCs on mineralized collagen scaffolds regardless of their composition increases overall osteogenic gene expression in both basal and licensed treatments. This increase in osteogenic gene expression following seeding was observed in *BGLAP*, *BMP2*, *COL1A2*, *MMP9*, *SOX9*, *SP7*, *TNFSF11*, and *WNT5a* for both chondroitin-6-sulfate and heparin compositions. However, licensed hMSCs displayed a greater overall osteogenic potential in early stages (days 3 and 7) which decreased with time. Licensed hMSCs expressed significantly ($p < 0.05$) different levels of both *BGLAP* and *BMP2* compared to basal hMSCs at day 3. Licensed cells on chondroitin-6-sulfate scaffolds expressed higher amounts of the *TNFSF11* gene compared with basal cells. Heparin containing scaffolds in both licensed and basal cell treatments displayed lower levels of the *TNFSF11* gene, which encodes for the RANK ligand (RANKL), a downstream osteoclast differentiation factor, compared to chondroitin-6-sulfate scaffolds. Heparin containing scaffolds displayed significantly lower ($p < 0.05$) levels of *BMP2* compared to chondroitin-6-sulfate containing scaffolds with basal cells at days 7 and 14. However this trend was not observed in other genes. Osteogenic gene levels within treatments largely showed no significance, and between treatments converged with time.

3.5. Immunomodulatory Gene Expression Is Driven by Initial Cell Inflammatory State and Is Independent of Scaffold Composition.

In our custom Nanostring panel, we investigated the expression of 13 immunomodulatory genes as a function of the cell initial inflammatory state and scaffold composition. Licensing hMSCs led the upregulation of all 13 immunomodulatory genes prior to seeding licensed cells onto the scaffolds (day 0) Figure 3C. At day 0, the highest expression was observed *in IDO1*, *CCL2*, *GAL9*, *TSG6*, *IL8*, and *IL6* ordered from highest with a 10-fold increase

compared to the basal cell gene expression, to lowest with 5.2-fold increase compared to basal cell gene expression. Following the seeding of licensed hMSCs on mineralized collagen scaffolds, we observed decreased immunomodulatory gene expression in 11 out of the 13 genes. The greatest decrease in expression was observed in *IDO1*, *CCL2*, and *GAL9* ranging from over 8 to 3 fold decrease in expression. However, the seeding of basal hMSCs on mineralized collagen scaffolds decreased the immunomodulatory gene expression of 5 out of the 13 genes, all common with ones in the licensed hMSCs (*CCL7*, *IDO1*, *IL8*, *IL6*, *PTGS2*, *TNFSF11A*). Basal hMSCs, although expressing lower levels of immunomodulatory genes in early stages of culture compared to licensed hMSCs, the expression of *CCL2*, *GAL9*, *HGF*, *IDO1*, *IL10*, *IL1RN*, *MCSF*, and *TSG6* increases with time, converging with the expression levels of licensed hMSCs by day 21. Licensed hMSCs express significantly ($p < 0.05$) higher levels of *TSG6*, *GAL9*, *IDO1*, and *IL6* compared to basal on day 3 and *CCL2* and *IL8* on days 3 and 7. Licensed hMSCs on heparin containing scaffolds displayed significantly ($p < 0.05$) increased *CCL2* gene expression compared to chondroitin-6-sulfate scaffolds on day 7. However, chondroitin-6-sulfate scaffolds displayed significantly ($p < 0.05$) increased *IL8* gene expression compared to heparin scaffolds on day 7. No further significance was observed for scaffold compositions within each treatment. At later stages of the study, including days 14 and 21, the immunomodulatory gene expression levels converged between treatments.

3.6. Pore Anisotropy Enhances hMSC Metabolic Activity Regardless of Basal or Licensed Conditions.

Since chondroitin-6-sulfate displayed the greatest promise in directing MSC responses toward a more immunomodulatory phenotype, we proceeded to compare scaffold pore architecture influences using CS6 as our glycosaminoglycan of choice. Licensing drove a higher metabolic activity in late stages of culture with significantly ($p < 0.05$) higher levels compared to basal cells at day 21 in anisotropic dependent manner (Figure 4A). However, scaffold pore anisotropy drove higher metabolic activity levels in early stages of culture. At day 14 of culture, anisotropic scaffolds with basal and licensed cells displayed significantly ($p < 0.05$) higher metabolic activity compared to the isotropic scaffolds seeded with basal cells.

3.7. hMSCs Seeded on Anisotropic Scaffolds Secrete Higher Amounts of Osteoprotegerin than Isotropic Scaffolds.

Licensing of MSCs significantly ($p < 0.05$) decreases OPG production compared to basal conditions on days 15 and 21 (Figure 4B). Anisotropic scaffolds seeded with basal cells expressed significantly higher ($p < 0.05$) amounts of OPG compared to isotropic scaffolds seeded with basal cells on days 15 and 21.

3.8. Licensed Cells Seeded on Mineralized Collagen Scaffolds Secrete Higher Amounts of Immunomodulatory Cytokines Compared to Basal Cells.

We observed that licensing drove a higher expression of PGE_2 and IL-6 compared to basal cells throughout the 21-day period in both scaffold groups (Figure 4C,D). Specifically, both isotropic and anisotropic scaffolds seeded with licensed cells showed significantly higher ($p < 0.05$) amounts of PGE_2 compared to basal groups on days 15 and 21. Although no

significance was determined, anisotropic scaffolds consistently expressed higher amounts of PGE_2 than do isotropic scaffolds. Furthermore, both isotropic and anisotropic scaffolds seeded with licensed cells showed significantly higher ($p < 0.05$) expression of IL-6 compared to the basal scaffold groups on day 15. However, there was no significance in both PGE_2 and IL-6 between scaffold groups of the same cell treatment throughout the 21-day culture.

3.9. Scaffold Anisotropy Does Not Influence Osteogenic Gene Expression.

Licensing hMSCs increases the overall osteogenic gene expression profile compared to basal cells in early stages of culture (day 3) Figure 5 A–B. Specifically, licensing increases *BMP2*, *COL1A2*, *MMP9*, *OPN*, and *TNFSF11* genes compared to basal cells. Seeding basal and licensed hMSCs on mineralized collagen scaffolds increased the levels of *BGLAP*, *BMP2*, *COL1A2*, *MMP9*, *SOX9*, *SP7*, *TNFSF11*, and *WNT5a* expression for both isotropic and anisotropic scaffolds in early stages of culture (day 3). The overall osteogenic potential in basal hMSCs was observed to be higher in isotropic scaffolds compared to anisotropic scaffolds however this was not observed for licensed hMSCs. Overall, licensing had a significant effect ($p < 0.05$) in early stages of the study (day 3) as seen in *BGLAP*, *BMP2*, and *MMP9* while scaffold architecture had no effect. Scaffold anisotropy did not display a significant effect on the overall osteogenic gene expression patterns. In the later stages of the study, the levels of osteogenic gene expression between basal and licensed cells converged.

3.10. Scaffold Structure Does Not Significantly Impact Immunomodulatory Gene Expression.

All immunomodulatory genes were up-regulated in licensed hMSCs prior to seeding (day 0). Following the seeding of licensed hMSCs on mineralized collagen scaffolds we observed a decrease in immunomodulatory gene expression for *IDO1*, *CCL2*, *GAL9*, *IL6*, *MCSF*, and *IL8* ranging in order from over 8- to 3-fold decrease in expression Figure 5C. However, despite the decrease from day 0 licensed hMSCs displayed significantly higher gene expression ($p < 0.05$) levels of *TSG6*, *IDO1*, and *IL6* compared to basal on day 3 of culture. Further, *GAL9*, *CCL2*, and *IL8* gene expression was significantly greater ($p < 0.05$) in licensed hMSCs on days 3 and 7 compared to basal hMSCs. Licensed hMSCs seeded on isotropic scaffolds displayed significantly higher amounts of *IDO1* on day 3, and *IL8* on day 7 ($p < 0.05$) compared to anisotropic scaffolds. However, no significance between scaffold structure was observed in early stages of culture within the basal groups. No significance was observed in later stages of culture and expression levels between treatments converged by day 21.

4. DISCUSSION

While MSCs may have been initially considered to help orchestrate tissue regeneration through lineage-specification and tissue biosynthesis, it is increasingly clear that their role in regenerative medicine may lie in their potential to locally regulate the activity of immune cells. Previous studies have defined the roles of biochemical signals and how they facilitate MSC immunomodulation and their subsequent ability to modulate immune cells such as monocytes and T cells.[5,36,37] However, evidence suggests MSCs are initially

benign and do not elicit immunomodulatory functions unless they are first activated or "licensed" by inflammatory cytokines[5] such as in the presence of interferon-γ (IFN-γ) and one or more other cytokines such as tumor necrosis factor (TNF), interleukin 1 alpha (IL-1a), or interleukin 1 beta (IL-1β). MSCs may then express high amounts of immunomodulatory mediators, such as prostaglandin E_2 (PGE_2) and interleukin-6 (IL-6). MSC-secreted PGE_2 has been shown to induce high levels of IL-10 production by macrophages, which is indicative of a transition toward an anti-inflammatory phenotype and lower levels of pro-inflammatory cytokines such as IL-12, TNF-α, IL-1β, and IL-23.[38–41] However, all of these studies have been conducted in 2D environments which have been shown to elicit significantly different responses to *in* vivo environments.[42] Specifically, 2D environments do not provide control over cell shape, which drives biophysical signals influencing cell bioactivities *in* vivo altering cell spreading, migration, and sensing of soluble factors. In the context of bone, 2D models lack significantly as they fail to mimic the native microenvironment as seen by the flattening of osteoblasts which changes the natural distribution of the cytoskeleton and alters their gene expression.[43,44] As a result, while numerous studies have focused on the effects of these immunomodulatory mediators on MSCs, the potential complicating role of the local extracellular matrix in MSC immunomodulation is the focus of our investigation.

Here, we show that mineralized collagen scaffold extracellular matrix signals can bias the degree of MSC osteogenic and immunomodulatory potential regulated by the initial inflammatory stimuli. We investigated the effect of glycosaminoglycan (GAG) type; chondroitin-6-sulfate (CS6) and heparin sulfate (Hep), and pore anisotropy; isotropic pores (Iso) and anisotropic pores (Ani) on regulating MSC osteogenic and immunomodulatory potential as a function of licensing with inflammatory factors IFN-γ and TNF-α. We have previously shown that chondroitin-6-sulfate scaffolds have a potential immunosuppressive and angiogenic capacity while heparin-containing scaffolds elicit the greatest osteogenic response.[29] We have further shown that anisotropic scaffolds elicit the greatest osteogenic response over longer culture periods compared to isotropic scaffolds.[23] The effects of the 3D extracellular matrix composition and structure as a function of the initial inflammatory state were determined through the analysis of the MSC secretome and a broad panel of osteogenic, immunomodulatory, and angiogenic genes. MSC metabolic activity provided insight into cell health and proliferation. Soluble osteoprotegerin (OPG) provided a metric of MSC osteogenic potential as OPG is a key osteoclast inhibitor, while soluble PGE_2 and IL-6 served as a metric of MSC immunomodulatory phenotype as they have been described as major effector molecules in the immunoregulatory effects of MSCs.[5,8–10] We also developed a broad panel of osteogenic, immunomodulatory, and angiogenic genes for investigation to gain further insight into the temporal effects of the extracellular matrix on MSC osteogenic and immunomodulatory behavior.

GAGs are major constituents of the organic ECM of bone and have been shown to intimately interact with signaling pathways and sequester growth factors, cytokines, and chemokines.[45,46] We have previously shown that increasing GAG sulfation within collagen scaffolds significantly impacts growth factor sequestration and enhanced tenocyte cell bioactivity.[47] We have further shown that mineralized collagen scaffolds allow for the sequential sequestration of growth factors prolonging their release profiles *in vitro*

suggesting the potential for temporal regulation of cellular activities critical to bone healing.[48] When comparing glycosaminoglycan types incorporated in mineralized collagen scaffolds, we have previously observed that although GAG content did not impact cell viability, heparin and chondroitin-6-sulfate-containing scaffolds increased mineral formation at the late stage of *in vitro* culture.[23] Separately, we further observed heparin containing scaffolds most significantly inhibit osteoclastogenesis via secreted osteoprotegerin (OPG).[29] We further observed that hMSC secretome generated by chondroitin-6-sulfate scaffolds reduced pro-inflammatory immune response and increased endothelial tube formation.[29]

Taking this knowledge into account, here we compare the influence of glycosaminoglycan type on biasing hMSCs toward an osteogenic or immunomodulatory phenotype in response to an initial inflammatory stimulus. We observed that the initial inflammatory stimuli did not have a significant effect on metabolic activity in early stages of culture, however in late stages, cells that had undergone licensing displayed a heightened metabolic activity (Figure 2A). Consistent with prior observations, MSCs in heparin-containing mineralized collagen scaffolds secreted higher levels of OPG in both basal and licensed treatment groups, with the basal groups expressing significantly more OPG than the licensed groups (Figure 2B). However, licensed hMSCs displayed an increased expression of immunomodulatory factors PGE_2 and IL-6 compared to basal hMSCs with those in chondroitin-6-sulfate scaffolds consistently releasing significantly more IL-6 than heparin containing scaffolds (Figure 2C,D). Taken together, this shows that while scaffolds containing heparin bias hMSCs toward an osteogenic phenotype regardless of initial inflammatory stimuli, scaffolds containing chondroitin-6-sulfate result in MSCs displaying greater immunomodulatory potential. Furthermore, mineralized collagen scaffolds regardless of glycosaminoglycan type, display a sustained immunomodulatory potential in licensed groups through the first 7 days of culture without the need for continuous inflammatory stimulation (Figure 3C). Gonzalez-Pujana et al. and Zimmermann et al. used heparin beads or nanoparticles conjugated with IFNγ respectively for the sustained delivery IFNγ.[7,36] Both observed that the sustained release of IFNγ led to the prolonged expression of immunomodulatory factors such as IDO and GAL9. Our findings hint to the potential of mineralized collagen scaffolds have the potential to elicit a prolonged immunomodulatory response from hMSCs while gradually suppressing the immune response to a basal state. While this work focused on the activity of MSCs after a single inflammatory priming event to establish the persistence of MSC response, there remains a significant opportunity to explore the use of prolonged inflammatory stimulation of hMSCs on mineralized collagen scaffolds to further elicit the regulating strength of heparin and chondroitin-6-sulfate.

Bone is a complex and highly porous composite structure, and the native anisotropy of trabecular bone is becoming increasingly explored in biomaterials fabrication. Petersen and others suggest that anisotropic pores in collagen biomaterials can promote intramembranous ossification, required in CMF bone repair.[49] We have previously explored the influences of pore anisotropy in mineralized collagen scaffolds on MSC osteogenic potential and observed that short-term MSC migration and activity was not affected by pore orientation, however, anisotropic scaffolds significantly increased bone mineral synthesis.[23] More recently, others employed anisotropy in the context of immunoregulation. McWhorter et al. employed a micropatterning approach to show substrate-induced elongation biased macrophages

toward an anti-inflammatory phenotype.[50] Su and others demonstrated that aligned fiber biomaterials have the greatest potential of immunomodulation via their paracrine functions promoting macrophage recruitment and polarization toward a pro-healing phenotype.[35,36] However, little is known about the influence of three-dimensional pore anisotropy on the MSC immunomodulatory potential. As chondroitin-6-sulfate-containing mineralized collagen scaffolds displayed the greatest promise in directing MSC responses toward a more immunomodulatory phenotype, we proceeded with CS6 as our GAG of choice. We observed that anisotropic scaffolds induced significantly greater metabolic activity in both basal and licensed groups in late stages of culture (Figure 4A). Agreeing with previous work, anisotropic scaffolds enhanced the secretion of OPG compared to isotropic scaffolds in late stages of culture with significantly higher levels observed in the basal hMSC group (Figure 4B). However, scaffold anisotropy did not significantly affect immunomodulatory potential, with MSC licensing the primary driver of immunomodulatory activity. We observed no significant differences in the expression of immunomodulatory factors PGE_2 and IL-6 between pore structure variants (Figure 4C,D). Similarly, no significant differences were observed in gene expression between pore structure variants (Figure 5). Interestingly, as seen with the glycosaminoglycan scaffolds, both structural variants exhibited a prolonged immunomodulatory potential through the first 7 days of culture without the need for repeated inflammatory stimuli. MSC licensing and adoption of an immunosuppressive phenotype are thought to be governed by the IFN-γ–JAK–STAT1 pathway.[51–53] It has been suggested that the influence of this pathway can be detected visually in the form of MSC morphological changes arising from actin polymerization, nuclear morphological shifts, and associated epigenetic modification.[51,54] Indeed, Klinker et al. observed that licensed MSCs displayed increased elongation and decreased nucleus-to-cytoplasm ratio. Additionally, the activation of NF-κB has been implicated in the activation of the MSC immunomodulatory phenotype, leading to downstream secretion of IL-6, CCL2, and other immunomodulatory molecules.[52,55,56] We hypothesize that the heightened secretions of IL-6 and PGE_2 that we observed in licensed MSCs during this study arise from the action of the IFN-γ–JAK–STAT1 pathway and from NF-κB activation. We further showed that both licensed and basal group immunomodulatory gene expression converged hinting to the immunosuppressive potential of mineralized collagen scaffolds. As such, future work will focus on identifying the effect of licensing MSCs on macrophage polarization as a function of mineralized collagen scaffolds to further elucidate the immunomodulatory capacity of our scaffolds.

MSCs are known to secrete a plethora of soluble factors directly influencing the cells in the surrounding microenvironment.[5,57] The plasticity of MSC-mediated immunomodulation has been previously shown in multiple studies and formally demonstrated as in a ‘chessboard titration’ of IFN-γ and TNF.[58] Here, we demonstrate the plasticity of MSCs in regard to both immunomodulatory and osteogenic activity. Notably, preconditioning MSCs with a single inflammatory stimulus event can significantly influence their osteogenic and immunomodulatory behavior across extended periods of culture. Interesting, key design parameters of mineralized collagen scaffolds (scaffold glycosaminoglycan content, pore anisotropy) provide extracellular signals that can increase MSC plasticity toward a more osteogenic and immunosuppressive state. Scaffold glycosaminoglycan content and pore structure have differential influences on the degree of this regulation, with heparin strongly

guiding MSCs toward an osteogenic phenotype, while MSCs in chondroitin-6-sulfate anisotropic scaffolds display a potentially immunomodulatory phenotype. Interestingly, the effect of pore anisotropy on hMSC immunomodulatory potential is not immediate, with overall hMSC activity most significantly established by the initial inflammatory challenge in the short term. However, others have shown that anisotropic structures on 2D substrates have the potential to influence macrophage polarization state.[50] Therefore, our findings suggest that the presence of immune cells such as macrophages and their inflammatory stimuli will differentially influence hMSC behavior as a function of pore anisotropy and glycosaminoglycan type respectively. Therefore, future work will focus on studying coculture influences of hMSCs with macrophages as a function of mineralized collagen scaffold extracellular matrix signals. Importantly, this work extends studies of the close relationship that exists between inflammation and regeneration through the use of a well-defined mineralized collagen scaffold with direct applications toward craniofacial bone repair.

5. CONCLUSIONS

MSC immunomodulation is gaining increasing attention in tissue engineering. However, most studies conducted to probe the influences of licensing on MSC immunomodulatory potential are done in 2D or in materials that do not mimic the native bone microenvironment. It is well established that 3D microenvironments have significantly different influences on cells than 2D environments and more closely mimic the native microenvironment.[59–61] Furthermore, the influence of initial inflammatory stimulation on MSC immunomodulation has been described; however, the influence of priming on osteogenic potential has yet to be studied. Here, we explored the influence of mineralized collagen scaffold extracellular matrix signals, namely, glycosaminoglycan type (chondroitin-6-sulfate or heparin) and pore anisotropy (isotropic or anisotropic) pores on hMSC immunomodulatory and osteogenic potential as a function of licensing. We demonstrated that licensing regulates hMSC phenotypic response toward an immunomodulatory phenotype. However, we showed that the glycosaminoglycan type can be harnessed to direct hMSC down an osteogenic phenotype by incorporating heparin or an immunomodulatory phenotype by incorporating chondroitin-6-sulfate. We further showed that pore anisotropy does not directly enhance hMSC immunomodulation, but rather the mineralized collagen scaffolds depict immunosuppressive potential. This work expands our understanding of the complex relationship between the immune response and regeneration and demonstrates a means to exploit this relationship through biomaterial design to ameliorate the immune response and enhance bone regeneration.

Supplementary Material

Refer to Web version on PubMed Central for supplementary material.

ACKNOWLEDGMENTS

The authors would like to acknowledge the Tumor Engineering and Phenotyping Shared Resource (TEP) at the Cancer Center at Illinois and Hui Xu for assistance with NanoString. The authors would also like to acknowledge the Harley Lab for assistance with reviewing the manuscript and results. The authors would also like

to acknowledge Dr. Kara Spiller for her valuable insight and discussion when conceptualizing this study. Additional support was provided by the Carl R. Woese Institute for Genomic Biology and the Chemical and Biomolecular Engineering Dept. at the University of Illinois at Urbana–Champaign. The interpretations and conclusions presented are those of the authors and are not necessarily endorsed by the National Institutes of Health or the National Science Foundation.

Funding

Research reported in this publication was supported by the National Institute of Dental and Craniofacial Research of the National Institutes of Health under Award Numbers R21 DE026582 and R01 DE030491 (BACH) as well as the National Institute of Arthritis and Musculoskeletal and Skin Diseases of the National Institutes of Health under Award Number R01 AR077858 (BACH). We are also grateful for funds provided by the NSF Graduate Research Fellowship (DGE-1746047, VK) and the Chemistry-Biology Interface Research Training Program at the University of Illinois (T32 GM070421, VK).

ABBREVIATIONS

CMF	craniomaxillofacial
hMSC or MSC	human mesenchymal stem cell
PGE_2	prostaglandin E_2
IL-6	Interleukin-6
IFNγ	Interferon gamma
TNFα	tumor necrosis factor alpha
OPG	osteoprotegerin
RANKL	RANK ligand
CS6 Iso	Isotropic chondroitin-6-sulfate mineralized collagen scaffold
Hep Iso	Isotropic heparin mineralized collagen scaffold
CS6 Ani	Anisotropic chondroitin-6-sulfate mineralized collagen scaffold
ALPL	alkaline phosphatase
BGLAP	Bone Gamma-Carboxyglutamate Protein
BMP2	Bone Morphogenetic Protein 2
BMP7	Bone Morphogenetic Protein 7
COL1A2	Collagen Type I Alpha 2 Chain
FGFR2	Fibroblast Growth Factor Receptor 2
IGF2	Insulin Like Growth Factor 2
IHH	Indian Hedgehog Signaling Molecule
MMP9	Matrix Metal-lopeptidase 9

OPN	Osteopontin
RUNX2	RUNX Family Transcription Factor 2
SEMA3A	Semaphorin 3A
SMAD5	SMAD Family Member 5
SOX9	SRY-Box Transcription Factor 9
SP7	Sp7 Transcription Factor
TNFSF11	TNF Superfamily Member 11
TNFRSF11B	TNF Receptor Superfamily Member 11b
WNT16	Wnt Family Member 16
WNT5a	Wnt Family Member 5A
CCL2	C-C Motif Chemokine Ligand 2
CCL7	C-C Motif Chemokine Ligand 7
GAL9	Galectin 9
HGF	Hepatocyte Growth Factor
IDO1	Indoleamine 2,3-Dioxygenase 1
IL-8	Interleukin 8
IL-10	Interleukin 10
IL1RN	Interleukin 1 Receptor Antagonist
IL-6	Interleukin 6
MCSF	Monocyte Colony Stimulating Factor
PTGS2	Prostaglandin-Endoperoxide Synthase 2
TNFRSF11A	TNF Receptor Superfamily Member 11a or RANK
TSG6	Tumor necrosis factor-inducible gene 6
ANGPT1	Angiopoietin 1
VEGFA	Vascular Endothelial Growth Factor A
VEGFB	Vascular Endothelial Growth Factor B
GAPDH	Glyceraldehyde-3-Phosphate Dehydrogenase
GUSB	Glucuronidase Beta
OAZ1	Ornithine Decarboxylase Antizyme 1

REFERENCES

(1). Greenwald AS; Boden SD; Goldberg VM; Khan Y; Laurencin CT; Rosier RN Bone-graft substitutes: facts, fictions, and applications. Journal of Bone and Joint Surgery 2001, 83 (2), 98–103.

(2). Ghanaati S; et al. Potential lack of ″standardized″ processing techniques for production of allogeneic and xenogeneic bone blocks for application in humans. Acta Biomater 2014, 10 (8), 3557–62. [PubMed: 24769111]

(3). Fretwurst T; et al. Comparison of four different allogeneic bone grafts for alveolar ridge reconstruction: a preliminary histologic and biochemical analysis. Oral Surg Oral Med Oral Pathol Oral Radiol 2014, 118 (4), 424–31. [PubMed: 25183228]

(4). Thompson EM; et al. Recapitulating endochondral ossification: a promising route to in vivo bone regeneration. Journal of tissue engineering and regenerative medicine 2015, 9 (8), 889–902. [PubMed: 24916192]

(5). Ferreira JR; et al. Mesenchymal Stromal Cell Secretome: Influencing Therapeutic Potential by Cellular Pre-conditioning. Front Immunol 2018, 9, 2837. [PubMed: 30564236]

(6). Li N; Hua J Interactions between mesenchymal stem cells and the immune system. Cell. Mol. Life Sci 2017, 74 (13), 2345–2360. [PubMed: 28214990]

(7). Gonzalez-Pujana A; et al. Multifunctional biomimetic hydrogel systems to boost the immunomodulatory potential of mesenchymal stromal cells. Biomaterials 2020, 257, 120266. [PubMed: 32763614]

(8). Wang Y; et al. Plasticity of mesenchymal stem cells in immunomodulation: pathological and therapeutic implications. Nature Immunology 2014, 15 (11), 1009–1016. [PubMed: 25329189]

(9). Lu D; et al. Mesenchymal Stem Cell-Macrophage Crosstalk and Maintenance of Inflammatory Microenvironment Homeostasis. Front Cell Dev Biol 2021, 9, 681171. [PubMed: 34249933]

(10). Kyurkchiev D; et al. Secretion of immunoregulatory cytokines by mesenchymal stem cells. World J Stem Cells 2014, 6 (5), 552–70. [PubMed: 25426252]

(11). Blaber SP; Webster RA; Hill CJ; Breen EJ; Kuah D; Vesey G; Herbert B. R Analysis of in vitro secretion profiles from adipose-derived cell populations. Journal of translational medicine 2012, 10 (1), 1–16. [PubMed: 22214470]

(12). Opal SM; DePalo VA Anti-inflammatory cytokines. Chest 2000, 117 (4), 1162–1172. [PubMed: 10767254]

(13). Ren X; et al. Nanoparticulate mineralized collagen scaffolds induce in vivo bone regeneration independent of progenitor cell loading or exogenous growth factor stimulation. Biomaterials 2016, 89, 67–78. [PubMed: 26950166]

(14). Weisgerber DW; Caliari SR; Harley BA Mineralized collagen scaffolds induce hMSC osteogenesis and matrix remodeling. Biomater Sci 2015, 3 (3), 533–42. [PubMed: 25937924]

(15). Kanungo BP; et al. Characterization of mineralized collagen-glycosaminoglycan scaffolds for bone regeneration. Acta Biomater 2008, 4 (3), 490–503. [PubMed: 18294943]

(16). Cunniffe GM; et al. Development and characterisation of a collagen nano-hydroxyapatite composite scaffold for bone tissue engineering. Journal of Materials Science: Materials in Medicine 2010, 21 (8), 2293–2298. [PubMed: 20091099]

(17). Al-Munajjed AA; et al. Development of a biomimetic collagen-hydroxyapatite scaffold for bone tissue engineering using a SBF immersion technique. J Biomed Mater Res B Appl Biomater 2009, 90 (2), 584–91. [PubMed: 19180526]

(18). Al-Munajjed AA; Gleeson JP; O'Brien FJ Development of a collagen calcium-phosphate scaffold as a novel bone graft substitute. Stud Health Technol Inform. 2008, 133, 11–20. [PubMed: 18376009]

(19). Harley BA; et al. Design of a multiphase osteochondral scaffold. II. Fabrication of a mineralized collagen–glycosaminoglycan scaffold. Journal of Biomedical Materials Research Part A: An Official Journal of The Society for Biomaterials, The Japanese Society for Biomaterials, and The Australian Society for Biomaterials and the Korean Society for Biomaterials 2009, 92 (3), 1066–1077.

(20). Lee JC; et al. Optimizing collagen scaffolds for bone engineering: effects of cross-linking and mineral content on structural contraction and osteogenesis. The Journal of craniofacial surgery 2015, 26 (6), 1992. [PubMed: 26147021]

(21). Lyons FG; et al. Novel microhydroxyapatite particles in a collagen scaffold: a bioactive bone void filler? Clin Orthop Relat Res 2014, 472 (4), 1318–28. [PubMed: 24385037]

(22). Wang X; et al. Restoration of a Critical Mandibular Bone Defect Using Human Alveolar Bone-Derived Stem Cells and Porous Nano-HA/Collagen/PLA Scaffold. Stem Cells Int 2016, 2016, 8741641. [PubMed: 27118977]

(23). Dewey MJ; et al. Anisotropic mineralized collagen scaffolds accelerate osteogenic response in a glycosaminoglycan-dependent fashion. RSC Adv 2020, 10 (26), 15629–15641. [PubMed: 32655857]

(24). Caliari SR; Harley BA Structural and biochemical modification of a collagen scaffold to selectively enhance MSC tenogenic, chondrogenic, and osteogenic differentiation. Advanced healthcare materials 2014, 3 (7), 1086–1096. [PubMed: 24574180]

(25). Caliari SR; Harley BAC The effect of anisotropic collagen-GAG scaffolds and growth factor supplementation on tendon cell recruitment, alignment, and metabolic activity. Biomaterials 2011, 32 (23), 5330–5340. [PubMed: 21550653]

(26). Caliari SR; Harley BAC Composite growth factor supplementation strategies to enhance tenocyte bioactivity in aligned collagen-GAG scaffolds. Tissue Engineering Part A 2013, 19 (9–10), 1100–1112. [PubMed: 23157454]

(27). Grier WK; Moy AS; Harley BAC Cyclic tensile strain enhances human mesenchymal stem cell Smad 2/3 activation and tenogenic differentiation in anisotropic collagen-glycosaminoglycan scaffolds. European cells & materials 2017, 33, 227. [PubMed: 28319248]

(28). Mozdzen LC; Thorpe SD; Screen HRC; Harley BAC The effect of gradations in mineral content, matrix alignment, and applied strain on human mesenchymal stem cell morphology within collagen biomaterials. Advanced healthcare materials 2016, 5 (14), 1731–1739. [PubMed: 27245787]

(29). Dewey MJ; Kolliopoulos V; Ngo MT; Harley BA Glycosaminoglycan content of a mineralized collagen scaffold promotes mesenchymal stem cell secretion of factors to modulate angiogenesis and monocyte differentiation: Scaffold GAG content influences MSC endogenous factor production. Materialia 2021, 18, 101149. [PubMed: 34368658]

(30). Ryan EJ; Bengtsson AK Immune function of the decoy receptor osteoprotegerin. Critical Reviews in Immunology 2002, 22 (3), 15.

(31). Ren X; Zhou Q; Foulad D; Tiffany AS; Dewey MJ; Bischoff D; Miller TA; Reid RR; He TC; Yamaguchi DT; Harley BA; et al. Osteoprotegerin reduces osteoclast resorption activity without affecting osteogenesis on nanoparticulate mineralized collagen scaffolds. Science advances 2019, 5 (6), No. eaaw4991.

(32). Harley BA; et al. Design of a multiphase osteochondral scaffold. II. Fabrication of a mineralized collagen-glycosaminoglycan scaffold. J Biomed Mater Res A 2009, 92 (3), 1066–77.

(33). Dewey MJ Glycosaminoglycan content of a mineralized collagen scaffold promotes mesenchymal stem cell secretion of factors to modulate angiogenesis and monocyte differentiation. Materialia (Oxf) 2021, 18, 101149. [PubMed: 34368658]

(34). O'Brien FJ; et al. The effect of pore size on cell adhesion in collagen-GAG scaffolds. Biomaterials 2005, 26 (4), 433–41. [PubMed: 15275817]

(35). Caliari SR; Harley BA The effect of anisotropic collagen-GAG scaffolds and growth factor supplementation on tendon cell recruitment, alignment, and metabolic activity. Biomaterials 2011, 32 (23), 5330–40. [PubMed: 21550653]

(36). Zimmermann JA; Hettiaratchi MH; McDevitt TC Enhanced Immunosuppression of T Cells by Sustained Presentation of Bioactive Interferon-gamma Within Three-Dimensional Mesenchymal Stem Cell Constructs. Stem Cells Transl Med 2017, 6 (1), 223–237. [PubMed: 28170190]

(37). Caplan AI Adult mesenchymal stem cells for tissue engineering versus regenerative medicine. J Cell Physiol 2007, 213 (2), 341–7. [PubMed: 17620285]

(38). Zhang QZ; et al. Human gingiva-derived mesenchymal stem cells elicit polarization of m2 macrophages and enhance cutaneous wound healing. Stem Cells 2010, 28 (10), 1856–68. [PubMed: 20734355]

(39). Cho DI; et al. Mesenchymal stem cells reciprocally regulate the M1/M2 balance in mouse bone marrow-derived macrophages. Exp Mol Med 2014, 46, No. e70.

(40). Francois M; et al. Human MSC suppression correlates with cytokine induction of indoleamine 2,3-dioxygenase and bystander M2 macrophage differentiation. Mol Ther 2012, 20 (1), 187–95. [PubMed: 21934657]

(41). Selleri S; Bifsha P; Civini S; Pacelli C; Dieng MM; Lemieux W; Jin P; Bazin R; Patey N; Marincola FM; Moldovan F; Zaouter C; Trudeau L-E; Benabdhalla B; Louis I; Beausejour C; Stroncek D; Le Deist F; Haddad E Human mesenchymal stromal cell-secreted lactate induces M2-macrophage differentiation by metabolic reprogramming. Oncotarget 2016, 7, 30193–30210. [PubMed: 27070086]

(42). Duval K; et al. Modeling Physiological Events in 2D vs. 3D Cell Culture. Physiology (Bethesda) 2017, 32 (4), 266–277. [PubMed: 28615311]

(43). Knight E; Przyborski S Advances in 3D cell culture technologies enabling tissue-like structures to be created in vitro. Journal of Anatomy 2015, 227 (6), 746–756. [PubMed: 25411113]

(44). Li Y; Kilian KA Bridging the Gap: From 2D Cell Culture to 3D Microengineered Extracellular Matrices. Advanced healthcare materials 2015, 4 (18), 2780–2796. [PubMed: 26592366]

(45). Salbach-Hirsch J New insights into the role of glycosaminoglycans in the endosteal bone microenvironment. Biol Chem 2021, 402, 1415. [PubMed: 34323057]

(46). Hachim D; et al. Glycosaminoglycan-based biomaterials for growth factor and cytokine delivery: Making the right choices. J. Controlled Release 2019, 313, 131–147.

(47). Hortensius RA; Harley BA The use of bioinspired alterations in the glycosaminoglycan content of collagen-GAG scaffolds to regulate cell activity. Biomaterials 2013, 34 (31), 7645–52. [PubMed: 23871542]

(48). Tiffany AS; Dewey MJ; Harley BAC Sequential sequestrations increase the incorporation and retention of multiple growth factors in mineralized collagen scaffolds. RSC Advances 2020, 10 (45), 26982–26996. [PubMed: 33767853]

(49). Petersen A; et al. A biomaterial with a channel-like pore architecture induces endochondral healing of bone defects. Nat Commun 2018, 9 (1), 4430. [PubMed: 30361486]

(50). McWhorter FY; et al. Modulation of macrophage phenotype by cell shape. Proc Natl Acad Sci U S A 2013, 110 (43), 17253–8. [PubMed: 24101477]

(51). Klinker MW; Marklein RA; Lo Surdo JL; Wei C-H; Bauer SR Morphological features of IFN-γ–stimulated mesenchymal stromal cells predict overall immunosuppressive capacity. Applied Biological Sciences 2017, 114 (13), No. E2598-E2607.

(52). Kim DS; Jang IK; Lee MW; Ko YJ; Lee D-H; Lee JW; Sung KW; Koo HH; Yoo KH Enhanced immunosuppressive properties of human mesenchymal stem cells primed by interferon-γ. EBioMedicine 2018, 28, 261–272. [PubMed: 29366627]

(53). Bach EA; Aguet M; Schreiber RD The IFNγ receptor: a paradigm for cytokine receptor signaling. Annual review of immunology 1997, 15 (1), 563–591.

(54). Rovira Gonzalez YI; Lynch PJ; Thompson EE; Stultz BG; Hursh DA In vitro cytokine licensing induces persistent permissive chromatin at the Indoleamine 2, 3-dioxygenase promoter. Cytotherapy 2016, 18 (9), 1114–1128. [PubMed: 27421739]

(55). Silva LHA; Antunes MA; Dos Santos CC; Weiss DJ; Cruz FF; Rocco PRM Strategies to improve the therapeutic effects of mesenchymal stromal cells in respiratory diseases. Stem Cell Research & Therapy 2018, 9 (1), 1–9. [PubMed: 29291747]

(56). Wong SW; Lenzini S; Cooper MH; Mooney DJ; Shin J-W Soft extracellular matrix enhances inflammatory activation of mesenchymal stromal cells to induce monocyte production and trafficking. Science advances 2020, 6 (15), No. eaaw0158.

(57). Bogatcheva NV; Coleman ME Conditioned Medium of Mesenchymal Stromal Cells: A New Class of Therapeutics. Biochemistry (Mosc) 2019, 84 (11), 1375–1389. [PubMed: 31760924]

(58). Li W; et al. Mesenchymal stem cells: a double-edged sword in regulating immune responses. Cell Death Differ. 2012, 19 (9), 1505–13. [PubMed: 22421969]

(59). Yuste I; Luciano FC; Gonzalez-Burgos E; Lalatsa A; Serrano DR Mimicking bone microenvironment: 2D and 3D in vitro models of human osteoblasts. Pharmacol. Res 2021, 169, 105626. [PubMed: 33892092]

(60). Duval K; Grover H; Han L-H; Mou Y; Pegoraro AF; Fredberg J; Chen Z Modeling physiological events in 2D vs. 3D cell culture. Physiology 2017, 32 (4), 266–277. [PubMed: 28615311]

(61). Antoni D; Burckel H; Josset E; Noel G Three-dimensional cell culture: a breakthrough in vivo. International journal of molecular sciences 2015, 16 (3), 5517–5527. [PubMed: 25768338]

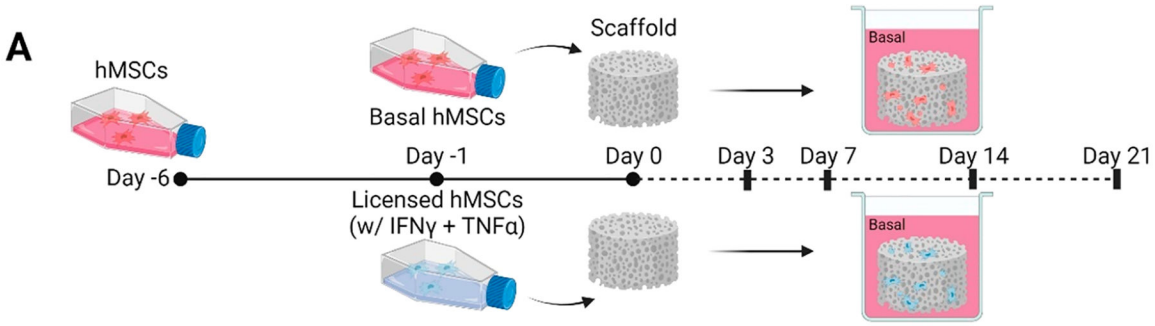

B

	Isotropic Chondroitin-6-sulfate (CS6)	Isotropic Heparin	Anisotropic Chondroitin-6-sulfate (CS6)
Mean pore size (μm)	T: 177 +/- 19.3 L: 169 +/- 5.2	~ Isotropic CS6	~ Isotropic CS6
Pore aspect ratio	T: 0.948 +/- 0.004 L: 0.955 +/- 0.003	~ Isotropic CS6	T: 0.887 +/- 0.034 L: 0.938 +/- 0.007
Elastic modulus	23.00 ± 0.6 kPa	~ Isotropic CS6	* > Isotropic CS6

Definitions: T: transverse, L: longitudinal, ~: no significant difference, *: significant difference ($p > 0.05$)

C

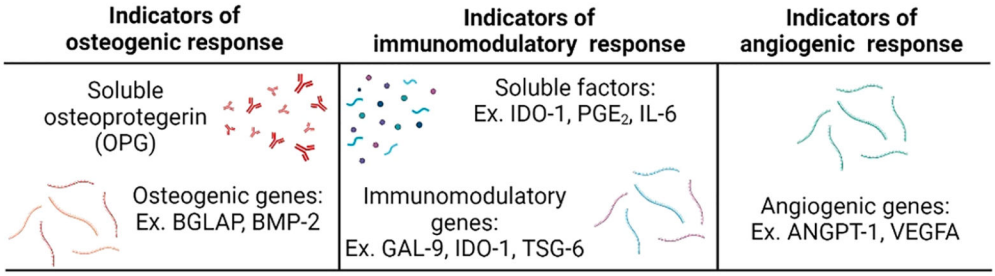

Figure 1.

(A) Experimental outline. MSCs licensed one day prior to seeding on mineralized collagen scaffolds and cultured for the duration of the study in basal conditions. Samples were collected for analysis on days 3, 7, 14, and 21. (B) Mineralized collagen scaffold property comparisons between glycosaminoglycan and pore anisotropy variants. (C) Metrics of osteogenic, immunomodulatory, and angiogenic responses used in this study.

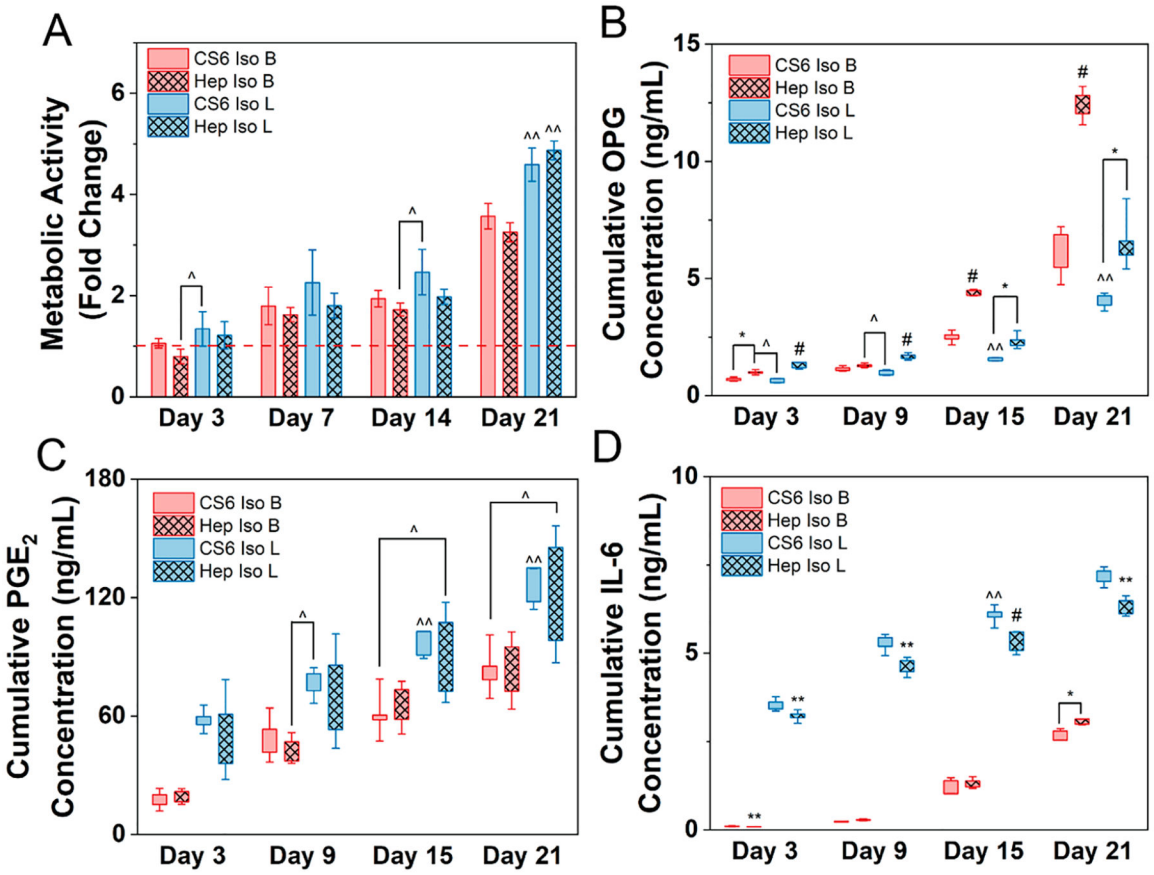

Figure 2.

Human mesenchymal stem cells (hMSCs) cultured in basal (B) or licensed (L) conditions were seeded on mineralized collagen scaffolds containing chondroitin-6-sulfate (CS6) or heparin (Hep) glycosaminoglycans with isotropic pores for 21 days in basal media. (A) Metabolic activity measured by nondestructive alamarBlue assay for each group over the 21-day culture period expressed as a fold change to a day 0 control for each treatment (basal or licensed), respectively ($n = 4$). Cumulative release of (B) osteoprotegerin - OPG, (C) prostaglandin E_2 - PGE2, and (D) interleukin 6 - IL-6 from hMSCs cultured in basal or licensed conditions seeded on mineralized collagen scaffolds over the 21-day period ($n = 5$). * denotes significance ($p < 0.05$) between indicated groups of same treatment (basal or licensed),** denotes significance ($p < 0.05$) between all groups of same treatment (basal or licensed),^ denotes significance ($p < 0.05$) between indicated groups of different treatment,^̂ denotes significance ($p < 0.05$) between indicated group and all other groups of other treatment, and # denotes significance ($p < 0.05$) of indicated group and all other groups at that time point.

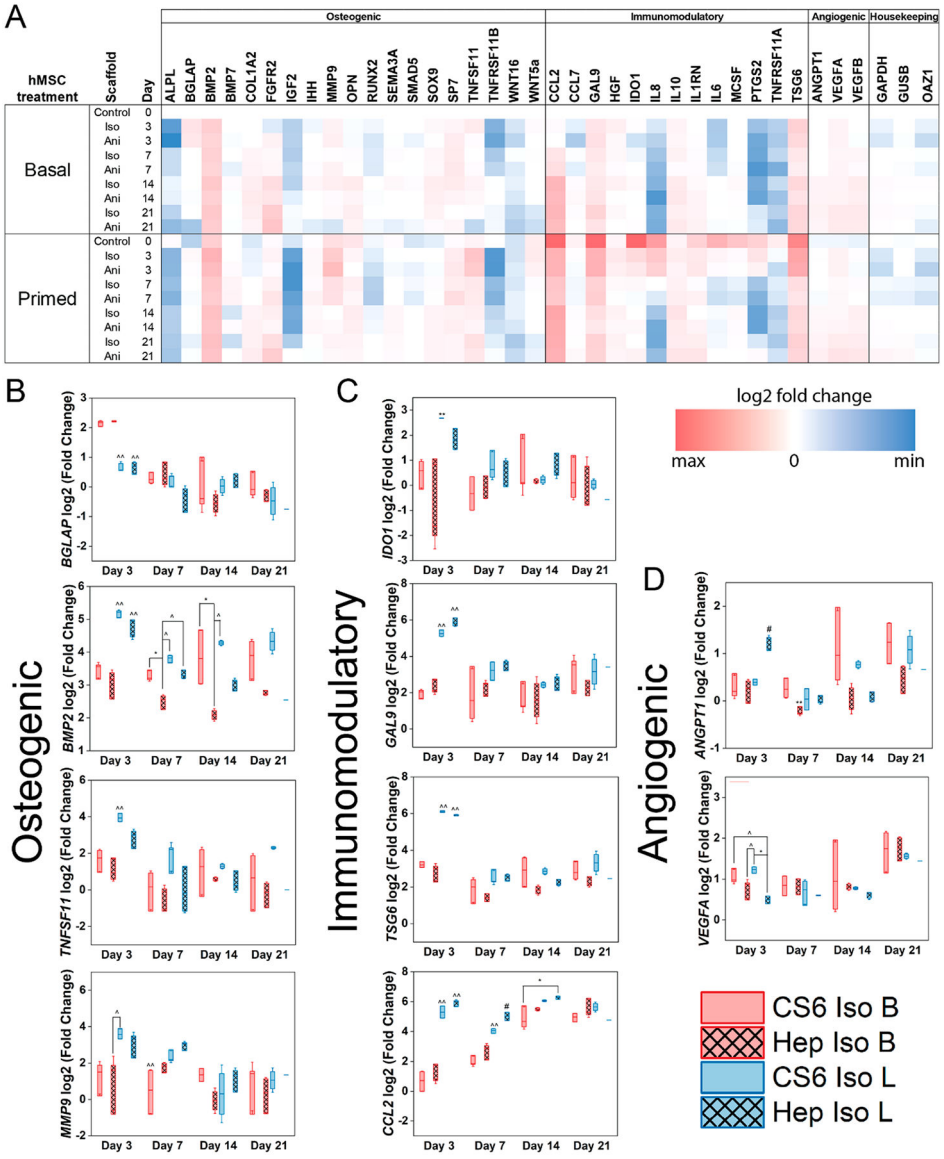

Figure 3.

(A) A custom NanoString code set was used to measure hMSC osteogenic and immunomodulatory and angiogenic gene expression in response to mineralized collagen scaffold glycosaminoglycan content (CS6; chondroitin-6-sulfate or Hep; heparin) as a function of initial culture conditions (basal - B or licensed - L). Gene expression is represented as a fold change compared to hMSC gene expression of basal cultured hMSCs prior to seeding ($n = 3$). (B) Subset of osteogenic genes (C) subset of immunomodulatory genes, (D) subset of angiogenic genes that displayed significance. * denotes significance ($p < 0.05$) between indicated groups of same treatment (basal or licensed), ** denotes significance ($p < 0.05$) between all groups of same treatment (basal or licensed),$^{\wedge}$ denotes significance ($p < 0.05$) between indicated groups of different treatment,$\hat{}$ denotes significance ($p < 0.05$) between indicated group and all other groups of other treatment, and # denotes significance ($p < 0.05$) of indicated group and all other groups at that time point.

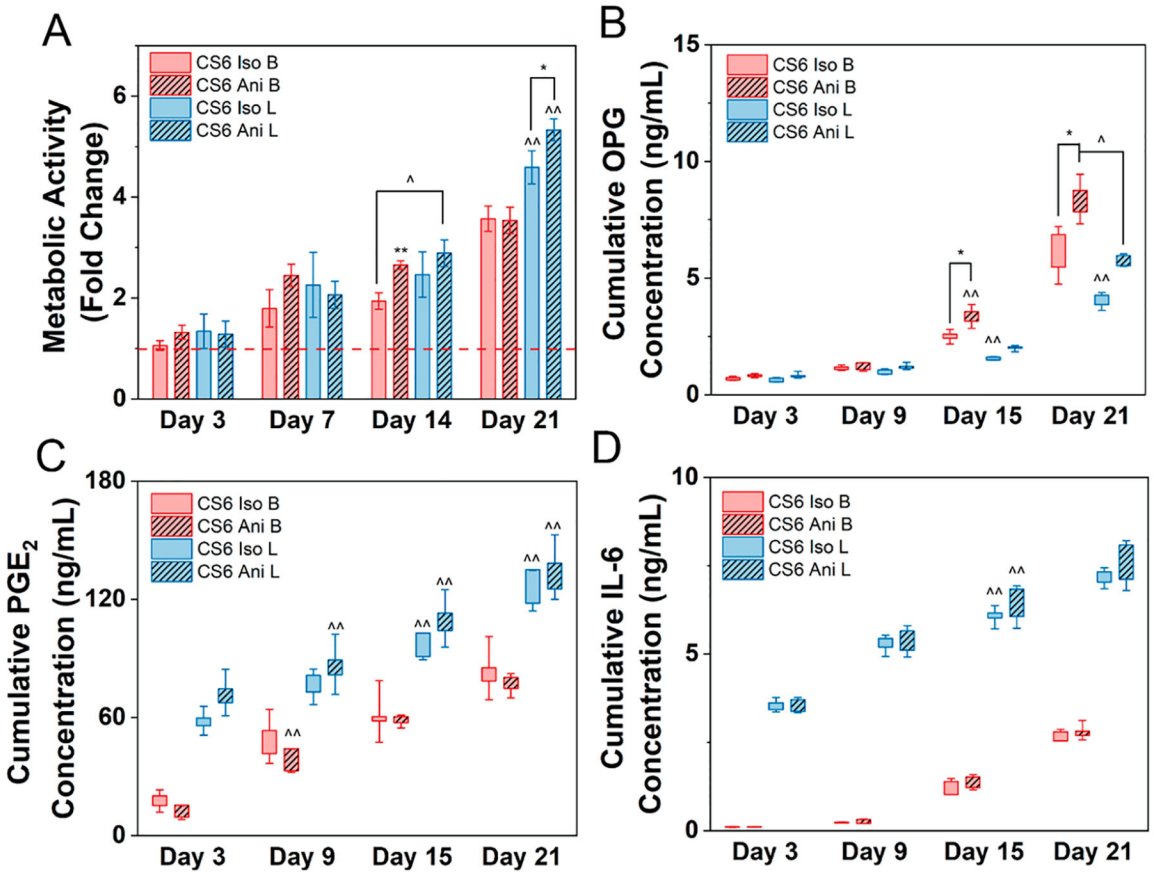

Figure 4.

Human mesenchymal stem cells (hMSCs) cultured in basal (B) or licensed (L) conditions were seeded on mineralized collagen scaffolds containing chondroitin-6-sulfate glycosaminoglycans with isotropic (Iso) or anisotropic (Ani) pores for 21 days in basal media. (A) Metabolic activity measured by nondestructive alamarBlue assay for each group over the 21-day culture period expressed as a fold change to a day 0 control for each treatment (basal or licensed), respectively ($n = 4$). Cumulative release of (B) osteoprotegerin - OPG, (C) prostaglandin E_2 - PGE_2, and (D) interleukin 6 - IL-6 from hMSCs cultured in basal or licensed conditions seeded on mineralized collagen scaffolds over the 21-day period ($n = 5$). * denotes significance ($p < 0.05$) between indicated groups of same treatment (basal or licensed), ** denotes significance ($p < 0.05$) between all groups of same treatment (basal or licensed),$\wedge$ denotes significance ($p < 0.05$) between indicated groups of different treatment,$\hat{\wedge}$ denotes significance ($p < 0.05$) between indicated group and all other groups of other treatment, and # denotes significance ($p < 0.05$) of indicated group and all other groups at that time point.

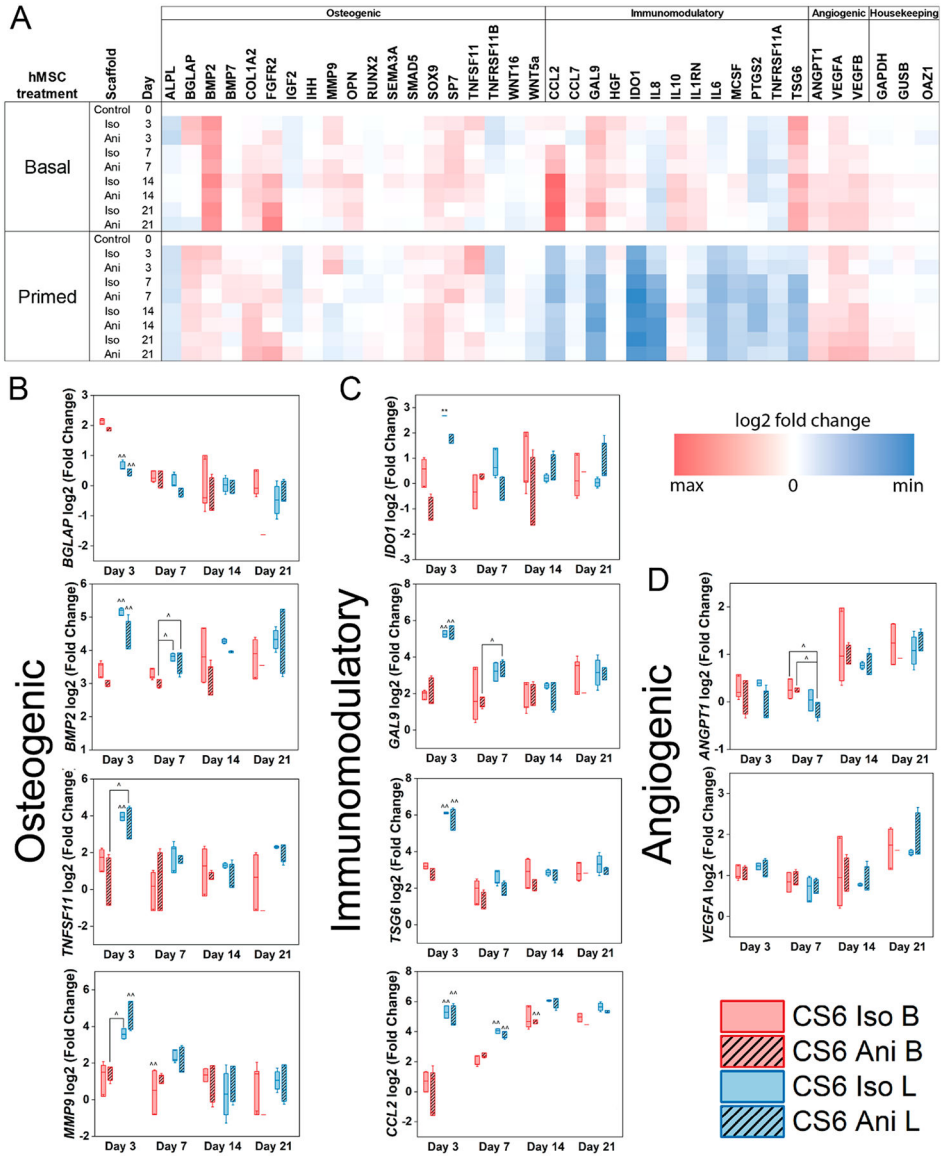

Figure 5.

(A) A custom NanoString code set was used to measure hMSC osteogenic and immunomodulatory and angiogenic gene expression in response to mineralized collagen scaffold pore structure (Iso; isotropic pores or Ani; anisotropic pores) as a function of initial culture conditions (basal - B or licensed - L). Gene expression is represented as a fold change compared to hMSC gene expression of basal cultured hMSCs prior to seeding (n = 3). (B) Subset of osteogenic genes (C) subset of immunomodulatory genes, (D) subset of angiogenic genes that displayed significance. * denotes significance ($p < 0.05$) between indicated groups of same treatment (basal or licensed), ** denotes significance ($p < 0.05$) between all groups of same treatment (basal or licensed),$^{\wedge}$ denotes significance ($p < 0.05$) between indicated groups of different treatment,$\hat{\wedge}$ denotes significance ($p < 0.05$) between indicated group and all other groups of other treatment, and # denotes significance ($p < 0.05$) of indicated group and all other groups at that time point.